From Decay to Rhythm: Sustained Biological Oscillators Require More Than Chemistry Alone

Yufei Wu[1,2] and Sean X. Sun[1,2,3]

[1]*Department of Mechanical Engineering, Johns Hopkins University, Baltimore, Maryland, USA*
[2]*Institute for NanoBioTechnology, Johns Hopkins University, Baltimore, Maryland, USA*
[3]*Center for Cell Dynamics, Johns Hopkins School of Medicine, Baltimore, Maryland, USA*

(Dated: April 15, 2025)

Many biological systems exhibit rhythmic oscillatory dynamics, yet it is shown that chemical reaction systems governed by Markovian dynamics cannot generate long-lasting oscillations. To overcome this limitation, we propose a general mechanism that couples a Markovian system to at least one other degree of freedom, such as a mechanical system, to achieve sustained oscillations with a desired frequency. We introduce two approaches, targeting different dynamical modes in the Markovian system, and derive a governing principle for the non-Markovian system by analyzing the eigenvalues of the coupled dynamics. This principle is validated using a trimolecular reaction system, successfully producing sustained oscillations. Our study provides theoretical insights into how any chemical system can be coupled to another non-Markovian system to produce sustained oscillations. We also make a fundamental observation that stability and control of stable limit cycles must arise from the non-Markovian part of the coupled system.

Introduction - One of the hallmarks of biological systems is the presence of sustained oscillatory dynamics [1–3]. Phenomena such as the heart beat [4], the cell cycle [5, 6], and the circadian rhythm [7, 8] are just a few examples where periodic dynamics are robust against external perturbations or changing environmental conditions. Recently, there have also been efforts to design oscillatory systems using tools of synthetic biology [9, 10]. Engineering these oscillatory systems and understanding natural biological oscillators require sound theoretical underpinning. Modeling of biological oscillators typically utilize kinetic rate equations describing multiple underlying chemical reactions and changes in densities of interacting components. For these types of models, conditions for establishing robust oscillatory dynamics are well known [11, 12]. However, it needs to be emphasized that kinetic rate equations (REs) are approximations to a more exact Markovian master equation description of kinetics [13]. The typical RE models that neglect fluctuations and higher order correlations are only first order moment approximations of Markovian dynamics. One can prove mathematically that Markovian dynamics cannot be the basis of sustained oscillations or limit cycles [14]. This statement implies that biological oscillatory dynamics cannot arise from biochemical reactions alone. Other types of interactions are necessary to generate sustained oscillations or limit cycles in biological systems.

We begin by demonstrating that sustained oscillations cannot emerge from Markovian dynamics. We then emphasize the distinction between the moment closure approach (i.e., REs) and the full Markovian dynamics as implemented by stochastic simulations. Using two autocatalytic chemical reactions in both open and closed systems, we show that oscillations predicted by the moment closure approximation disappear when they are described more accurately by continuous-time Markovian dynamics. This discrepancy arises due to the truncation of higher-order moments in an expansion of the master equation.

To achieve sustained oscillations, a chemical system must be coupled to at least one other degree of freedom. We show that coupling a Markovian system with an unstable non-Markovian system (e.g., a mechanical system) can restore sustained oscillations. We propose two approaches targeting distinct dynamical modes in the Markovian system: direct decay and oscillatory decay. By analyzing the eigenvalues of the coupled Markovian and non-Markovian system, we derive a design principle for the non-Markovian component to enable sustained oscillations. This principle is validated using a trimolecular reaction system, where we successfully achieve sustained oscillations with the desired frequency. Our study enhances the understanding of sustained oscillations in biological systems, emphasizes the role of the non-Markovian component in oscillatory behavior, and provides theoretical insights into the design and control of stable biological oscillators.

Continuous-time Markovian models are inadequate for sustained oscillations - For a continuous-time Markov chain, the time evolution of the probabilities of n distinct states is governed by the master equation:

$$\frac{\partial \mathbf{P}}{dt} = \mathbf{M} \cdot \mathbf{P} \tag{1}$$

where $\mathbf{P}(t)$ is an n-dimensional vector denoting the probabilities of all n states at time t. The off-diagonal elements of the "transition matrix", $\mathbf{M}_{\beta\alpha} \equiv k_{\alpha\to\beta}$, is the probability per unit time to jump from the state α to β. The diagonal elements $\mathbf{M}_{\alpha\alpha} \equiv -K_\alpha$ denotes the net escape rate from the state α. Because of the conservation of probability, all elements of $\mathbf{M}$ satisfy: $\sum_\alpha \mathbf{M}_{\alpha\beta} = 0$, and all diagonal elements are negative. Given this spe-

cific property, it can be proven that the real part of all non-zero eigenvalues of $\mathbf{M}$ are negative [14] (Supplemental Material, SM). This implies that $\mathbf{P}$ for any state must be a decaying function of time, which proves that continuous-time Markov systems can not generate sustained oscillation or limit cycles. This conclusion holds regardless of whether the waiting time between jumps follows an exponential distribution characterized by a constant rate $k_{\alpha\to\beta}$, or a more complex distribution.

Relationship between rate equations and the master equation - It has been noted that Markovian dynamics in Eq. 1 is the most fundamental description of chemical reactions [13]. A "state" in a reaction system is labeled by the number of various interacting species. Each reaction is a stochastic jump that changes the state or the number of reactant/products. This concept can be presented in a general form of the chemical master equation, described in [15]. We roughly sketch the theoretical framework here. Consider a chemical reaction network with N different molecule species and R chemical reactions. The reactions can be generally described by sets of chemical equations:

$$\sum_{i=1}^{N} s_{ij} X_i \xrightarrow{k_j} \sum_{i=1}^{N} r_{ij} X_i, j = 1, \ldots, R \tag{2}$$

where X_i is the number of molecule i, s_{ij} and r_{ij} are the stoichiometric coefficients of reactants and products respectively. The specific form of chemical master equations can be written as:

$$\frac{\partial P(\mathbf{n},t)}{\partial t} = \sum_{i=1}^{R} [a_i(\mathbf{n}-S_i)P(\mathbf{n}-S_i,t) - a_i(\mathbf{n})P(\mathbf{n},t)] \tag{3}$$

where $P(\mathbf{n},t)$ is the probability of finding molecules with numbers $\mathbf{n}$ at time t. a_i is the propensity function of reaction i, which depends on the concentration of the reactants. S is the net stoichiometric matrix which is defined as: $S_{ij} = r_{ij} - s_{ij}$, where S_i is the ith column of matrix S. The standard approach for simulating the chemical master equation is the stochastic simulation algorithm (SSA), such as the Gillespie algorithm [16, 17]. However, due to the high computational cost associated with large systems, an alternative method is the moment closure approximation [18]. In this approach, instead of considering the full probability of each state, only moments of the probability distribution are analyzed. The moment equations can be written as:

$$\frac{d\mu_i}{dt} = \sum n_1^{i_1} \ldots n_N^{i_N} \frac{dP(\mathbf{n},t)}{dt} = \sum_r \sum_{|j|=0}^{|i|-1} \prod_{k=1}^{N} \binom{i_k}{j_k} S_{kr}^{i_k - j_k} \langle a_r(n) \prod_{l=1}^{N} n_l^{j_l} \rangle \tag{4}$$

Here, μ_i represents the ith-order moment: $\mu_i = \langle \prod_{k=1}^{N} n_k^{i_k} \rangle$. The multi-index notation is expressed as: $\sum_{|j|=0}^{|i|-1} = \sum_{0\le j_l \le i_l (l=1,\ldots,N), 0 \le \sum_{l=1}^{N} j_l \le |i|-1}$. Details of the derivation and implementation are provided in reference [19, 20]. The moment equations are nonlinear ODEs. To close the series of moment equations, it must be truncated at a finite order q. The choice of closure depends on the system, common options including zero closure, normal closure, log-normal closure, among others [18]. Notably, the typical REs correspond to the moment closure scheme truncated at the first order, or the mean of the full probability distribution. This implies that REs generally neglect fluctuations and higher order correlations.

Archetypal chemical oscillators in open and closed systems - In this section, we present two examples that highlight the inability of Markov systems to generate sustained oscillations. We examine parameter regimes where oscillations are predicted by the approximate REs and compare RE solutions with those obtained from the stochastic simulation algorithm.

A classic "chemical oscillator" is the Brusselator [21], a paradigmatic model of nonlinear autocatalytic reactions in open systems (Fig. 1a). This system involves two species, X and Y, and is governed by the following reactions:

$$2\,\mathrm{X} + \mathrm{Y} \xrightarrow{\mathrm{c}_1/\Omega^2} 3\,\mathrm{X}, \mathrm{X} \xrightarrow{\mathrm{c}_2} \mathrm{Y}, \mathrm{A} \underset{\mathrm{c}_4}{\overset{\mathrm{c}_3\,\Omega}{\rightleftharpoons}} \mathrm{X} \tag{5}$$

where c_1, c_2, c_3, c_4 are the reaction constants, and Ω is a system-size parameter. The concentration of molecule A is fixed, which is incorporated into the constant c_3. Reaction 5 is solved using both the Gillespie algorithm and moment closure approximation (up to 5th order). We compare the results of widely used REs (first-order moment closure) with stochastic simulation results for a small system size, where the initial molecule numbers are $X = 1, Y = 1$. In the parameter regime where oscillations are observed in REs, the stochastic simulations instead show decay (Fig. 1b). In the phase portraits, REs exhibit a limit cycle, while stochastic simulations show an attractor-like behavior (Fig. 1c). Higher-order moment closure (zero closure scheme) produces more accurate re-

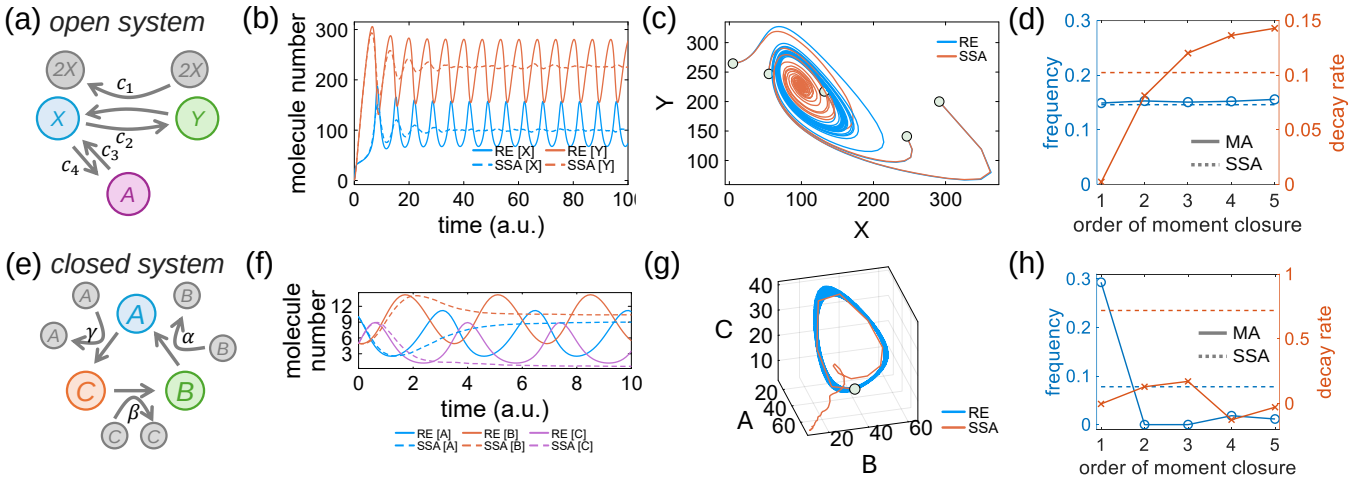

FIG. 1: Intrinsic stability of Markovian systems, which cannot generate sustained oscillations. (a) The Brusselator: an autocatalytic chemical oscillator in an open system. (b) Time evolution of molecular populations obtained from rate equations (REs) and the stochastic simulation algorithm (SSA). REs are obtained from first-order moment closure approximation. REs can generate sustained oscillations but fail to capture the decaying nature of the full dynamics described by the Stochastic Simulation Algorithm (SSA). (c) Phase portraits of molecular populations: RE produces a limit cycle, whereas SSA simulations reveal decaying oscillations. (d) Frequency and decay rates derived from various orders of moment closure approximations (MAs) and SSA simulations. MAs accurately predict oscillation frequencies but fail to capture decay rates. (e) A trimolecular autocatalytic reaction in a closed system with fixed number of molecules. (f) Temporal dynamics of molecular populations from RE and SSA simulations. (g) Phase portraits for the closed system without backward reactions, SSA results suggest that the system tends to evolve to a single-species steady state. (h) Frequency and decay rates derived from MAs and SSA simulations, highlighting the inability of MAs to accurately approximate either property in a closed system. In both examples, we use the "central-moment-neglect" approximation for the moment closure [19].

sults [18]. An additional point of interest is whether moment closure approximations can accurately predict both the oscillation frequency and the decay rate with increasing order of closure. For the Brusselator, moment closure approximations of all orders provide relatively accurate predictions for the oscillation frequency but fail to predict the decay rate correctly (Fig. 1d). Notably, an accurate frequency prediction and converging but incorrect decay rate for REs are characteristics of open systems with an infinite supply of reactants. This behavior contrasts with what is observed in closed systems. The decaying property of oscillations is also examined in another example of a "biological oscillator" featuring the tumor suppressor P53, which involves feedbacks in a reaction network of an open system (SM, Fig. S1).

The previous example explores an open system with infinite pool of reactants. However, biological systems are finite and cells have a limited number of interacting proteins. To investigate this, we examine a minimal closed system exhibiting oscillatory behavior described by REs. This system involves three species (Fig. 1e), with the following reactions:

$$\mathrm{A} + \mathrm{B} \xrightarrow{\alpha} 2\,\mathrm{A}, \mathrm{B} + \mathrm{C} \xrightarrow{\beta} 2\,\mathrm{B}, \mathrm{C} + \mathrm{A} \xrightarrow{\gamma} 2\,\mathrm{C} \qquad (6)$$

where k_1, k_2, and k_3 represent the reaction rate constants. In this closed system, the total number of A, B, and C remains constant over time. We simulate this system starting with the state $n_A = 10, n_B = 5, n_C = 5$. Fig. 1f-g shows that although REs predict sustained oscillation, the real dynamics show decay behavior and a stable steady state. Unlike the Brusselator, which is an open system, REs for this reaction do not provide satisfactory predictions for either the oscillation frequency nor the decay rate (Fig. 1h). This is an important feature of closed systems where the total molecular number is fixed and small, and the system only contains forward reactions. In such processes, it is easy to reach a state where only one molecule remains, leading to a steady-state probability distribution concentrated at three states, each representing a single molecule type. This characteristic renders the commonly used moment closure schemes ineffective, as the probability distribution is not accurately captured by analytical distribution functions. These examples confirm that pure Markov systems cannot generate true oscillations. Sustained oscillations predicted in simple Markov models arise from errors in moment closure approximations. So, how do biological systems, such as the circadian rhythm, generate sustained oscillations with precise and robust frequencies?

Coupling a Markov system with an unstable non-Markov system generates sustained oscillations - In order to achieve sustained oscillation, it is necessary to in-

troduce another degree of freedom that influences the probability of each state to mitigate the decay in Markov systems. In this study, we show a specific realization by coupling the stable Markov system to an unstable non-Markov system (Fig. 2) (a control input). This type of models appears in many multi-physics models of biological systems such as the Hodgkin-Huxley model [22], which couples ion channel opening probabilities with cell membrane voltage. While ion transport via ion channels follows a Markov process described by the master equation, the electrical potential is governed by membrane capacitance and therefore does not follow Markovian dynamics (SM).

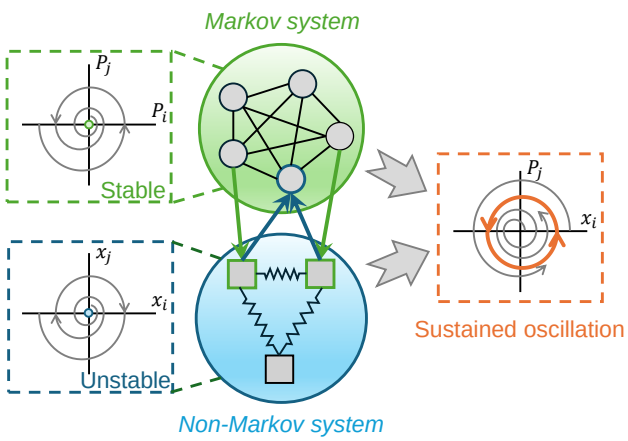

FIG. 2: Coupling a stable Markov system to an unstable non-Markov system can generate sustained oscillation.

In the most general form, we can write the linearized governing equation for the coupled system as (SM):

$$\frac{\partial \mathbf{P}}{\partial t} = \mathbf{M} \cdot \mathbf{P} + \mathbf{B}_1 \cdot \mathbf{x} \tag{7}$$

$$\frac{\partial \mathbf{x}}{\partial t} = \mathbf{B}_2 \cdot \mathbf{P} + \mathbf{C} \cdot \mathbf{x} \tag{8}$$

where $\mathbf{P}$ is a n dimensional vector that denotes the probability of each state in the Markov system while $\mathbf{x}$ is a l dimensional vector which is the state variable of the coupled system (e.g., a mechanical system). Consequently, the coupling matrices $\mathbf{B}_1$ and $\mathbf{B}_2$ are with dimensions $n \times l$ and $l \times n$. In order to maintain probability conservation, $\mathbf{B}_1$ should satisfy: $\sum_i \mathbf{B}_{1,ij} = 0$. The matrices $(\mathbf{M}, \mathbf{B}_1, \mathbf{B}_2, \mathbf{C})$ forms an overall $(n+l) \times (n+l)$ matrix $\mathbf{A}$. An analytical solution for the input variable $\mathbf{x}$ can be expressed in terms of $\mathbf{P}$ as:

$$\mathbf{x}(t) = e^{t\mathbf{C}} \cdot \mathbf{x}(0) + e^{t\mathbf{C}} \cdot \int_0^t e^{-s\mathbf{C}} \cdot \mathbf{B_2} \cdot \mathbf{P}(s) ds \tag{9}$$

We see that $\mathbf{x}(t)$ is an integral of the probability $\mathbf{P}(t)$, which is also the concept behind an integral controller [23]. For the purpose of generating sustained oscillations, we seek to design coupling matrices $\mathbf{B}_1, \mathbf{B}_2$, such that $(\mathbf{A})$ has at least one eigenvalue with zero real part and non-zero imaginary part. To prevent instability, we also require that the real parts of other eigenvalues are non-positive. Denoting the new eigenvalues of $\mathbf{A}$ as λ, the characteristic equations are:

$$\prod_{i \in S_1} \left(\sigma_i^{(1)} - \lambda - \frac{q_i^{(1)} q_i^{(2)}}{\sigma_i^{(2)} - \lambda} \right) \prod_{j \in S_2} \det \left[\mathbf{D}_{1,jj} - \lambda \mathbf{I} - \mathrm{diag} \left(\frac{q_\alpha^{(1)} q_\alpha^{(2)}}{\sigma_\alpha^{(2)} - \lambda}, \frac{q_\beta^{(1)} q_\beta^{(2)}}{\sigma_\beta^{(2)} - \lambda} \right) \right] = 0 \tag{10}$$

Here $\sigma_i^{(1)}, \sigma_i^{(2)}$ are the real eigenvalues of matrices $\mathbf{M}$ and $\mathbf{C}$. $\sigma_i^{(1)}$ excludes the inherent zero eigenvalue in $\mathbf{M}$. $\mathbf{D}_1$ is a quasi-upper triangular matrix of $\mathbf{M}$ after Schur decomposition. The diagonal blocks are either scalar or 2 by 2 matrices. For convenience, all matrix blocks are placed at the bottom right, denoted by $\mathbf{D}_{1,jj}$. $q_i^{(1)} q_i^{(2)}$ describes the coupling strength between the Markov and non-Markov systems. Detailed derivation is in the SM. S_1 is the set of positional indices of scalar diagonal elements in $\mathbf{D}_1$, S_2 is the set of positional indices corresponding to 2×2 blocks in $\mathbf{D}_1$. α, β are the indices of individual scalar entries corresponding to the jth block.

From Eq. 10, we observe two approaches that can both achieve pure imaginary eigenvalues corresponding to sustained oscillations. The first approach targets the real eigenvalues of the Markov system (first product in Eq. 10), while the second targets the complex eigenvalues (second product, Fig. S3). These approaches lead to different dynamical transitions. The first approach turns a stable non-oscillatory mode into a sustained oscillatory mode, while the second turns a decaying oscillatory mode into a sustained one. For the first approach, the condition for eigenvalues with zero real part is $\sigma_i^{(1)} + \sigma_i^{(2)} = 0$ and $\sigma_i^{(1)} \sigma_i^{(2)} - q_i^{(1)} q_i^{(2)} > 0$. For the other eigenvalues, the real part of λ should be non-positive. The frequency of the coupled system is $\omega = \sqrt{\sigma_i^{(1)} \sigma_i^{(2)} - q_i^{(1)} q_i^{(2)}}$.

The condition for sustained oscillation can be interpreted as follows: Since the Markovian system always has negative real eigenvalues ($\sigma_i^{(1)} < 0$), $\sigma_i^{(2)} > 0$ must hold, implying that the non-Markovian system should be inherently unstable. Additionally, $\sigma_i^{(1)}\sigma_i^{(2)} - q_i^{(1)}q_i^{(2)} > 0$ requires $-q_i^{(1)}q_i^{(2)}$ to be large enough to make this term positive. This means that: 1. There must be strong coupling between the two systems. 2. The systems must influence each other in opposite directions (e.g., A inhibits B while B enhances A), i.e., a negative feedback loop, a common feature observed in oscillatory systems [24, 25]. When the non-Markovian system targets the complex eigenvalues of the Markov matrix, the second product in Eq. 10 must generate pure imaginary roots. Denoting individual elements of $\mathbf{D}_{1,ii}$ as $d_{\alpha\beta}$ ($i \in S_2$), the new eigenvalues λ of the coupled system can be solved from:

$$\left[d_{\alpha\alpha}^{(1)} - \lambda - \frac{q_\alpha^{(1)}q_\alpha^{(2)}}{\sigma_\alpha^{(2)} - \lambda}\right]\left[d_{\beta\beta}^{(1)} - \lambda - \frac{q_\beta^{(1)}q_\beta^{(2)}}{\sigma_\beta^{(2)} - \lambda}\right] - d_{\alpha\beta}^{(1)}d_{\beta\alpha}^{(1)} = 0 \tag{11}$$

Eq. (11) is a quartic equation with four roots. Assuming the βth element in the non-Markovian system is weakly coupled to the Markov system, we can approximate $q_\beta^{(1)} = 0$. This decouples one dimension, reducing the quartic equation to a cubic of the form $a\lambda^3 + b\lambda^2 + c\lambda + d = 0$. For the equation to have pure imaginary roots, the necessary and sufficient conditions are $bc = ad$ and $b > 0$, $c > 0$.

Example - generating sustained oscillation in a trimolecular reaction by designing a coupled non-Markovian system - We use a trimolecular reaction as an example to design a coupled system that generates sustained oscillations (Fig. 3a). Results from the full master equation are given in the SM. Starting with 20 molecules, we have 231 states (Fig. S2). The coupled system is described by Eqs. 7 - 8. For illustration, we design a simple one-dimensional input, $x(t)$, targeting the largest nonzero real eigenvalue of matrix $\mathbf{M}$. The dynamical results are shown in Fig. 3b. Coupling with a non-Markovian system can generate sustained oscillations and transition from a decaying to an oscillatory dynamical mode.

Results show that it is possible to design an oscillator with a targeted frequency by adjusting the eigenvalue of the coupled system ($\sigma_i^{(2)}$) and coupling coefficients ($q_i^{(1)}, q_i^{(2)}$) according to Eq. 10. As discussed previously, the Markovian system has two dynamical modes: a direct decaying mode (real eigenvalue) and an oscillatory decaying mode (complex eigenvalues). Targeting the direct decaying mode in the non-Markovian system transforms the decaying process into a sustained oscillation. The obtained frequency as a function of ($\sigma_i^{(2)}, q_i^{(1)}q_i^{(2)}$) is illustrated in a phase diagram (Fig. 3c) with four regions (I-IV). Generating sustained oscillations requires precise eigenvalue design, as the system becomes either stable or unstable when the eigenvalue is too small or too large. The coupling effects ($q_i^{(1)}, q_i^{(2)}$) further categorize the system into oscillatory or non-oscillatory states. A strong negative coupling between the systems is required for sustained oscillations, as outlined in the previous section. Fig. S4 demonstrates the accuracy of our design within a target frequency. Multiple frequency components can be generated by coupling to different modes in the Markov system, giving various wave shapes. However, as the system dimension increases, the predictions become more sensitive to noise and perturbations. The larger matrices involved lead to higher errors in eigenvalue calculations, impacting accuracy of results (Fig. S5).

Similarly, we can obtain a frequency phase diagram when the non-Markov system is targeting the oscillatory decaying mode in the Markov system (corresponding to complex eigenvalues). This transforms a decaying oscillatory mode to a sustained oscillatory mode. Here, we take the assumption made in the previous section that the two by two matrix in the non-Markov system corresponding to the targeting mode in Markov system has one eigenvalue much larger than the other, denoted by $\sigma^{(2)}$. A more complex phase diagram is seen in Fig. 3d.

When targeting the oscillatory decay mode, in addition to designing a system with a preferred frequency, we can also eliminate certain frequency components from the original Markov system (Fig. 3d). For example, we can introduce a positive coupling ($q^{(1)}q^{(2)} > 0$) to change an oscillating mode in the original Markov system to a non-oscillatory one (Upper Regions I&II).

Generating biological limit cycles - It is important to note that strictly speaking, sustained oscillations generated by Eq. (7-8) are not true limit cycles, i.e., stable trajectories in phase space that attract nearby trajectories. A necessary condition for generating a limit cycle is nonlinearity. However, since the Markovian chemical system is intrinsically linear, we see that a necessary design principle is that the non-Markovian system must provide the sources of stability. For example, a cubic term can be introduced in the equation for $\mathbf{x}$ in Eq. (8). This is also what is observed in the Hodgkin-Huxley model.

Conclusion and discussion - In this paper, we demonstrate that the Markovian master equation, commonly used to model chemical reaction systems, cannot generate sustained oscillations. While many studies acknowledge the decaying nature of Markovian dynamics, they often neglect it, which is reasonable for short time scales. However, in processes such as circadian rhythms and cell cycle progression, where the time scale is much longer, we show that an additional non-Markovian input is necessary to prevent oscillation decay. One such example is the Hodgkin-Huxley model, which couples ion channel dynamics with the membrane voltage, the membrane voltage influence ion channel dynamics, and is not Markovian. This system is able to generate sustained oscillatory behavior that leads to action potentials [26]. Similarly,

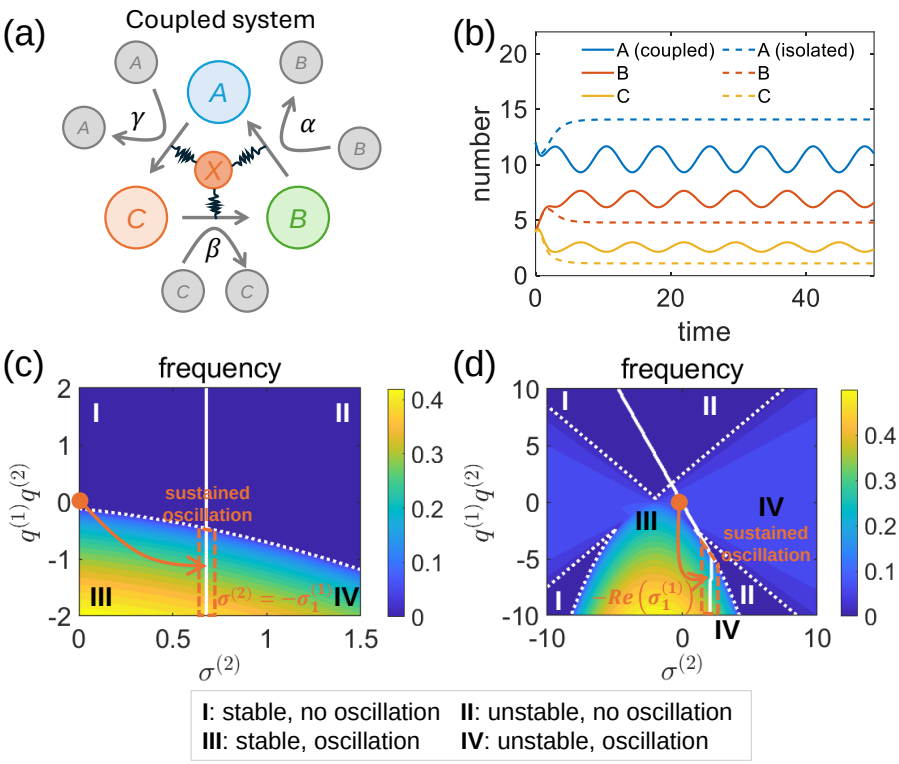

FIG. 3: Generation of sustained oscillations in a trimolecular reaction system. (a) Schematic representation of the coupled oscillatory system. (b) Temporal evolution of molecular populations in the isolated Markov system and the coupled oscillatory system. (c) Phase diagram illustrating system dynamics as a function of the eigenvalues of the non-Markov system ($\sigma^{(2)}$) and coupling coefficients ($q^{(1)}q^{(2)}$). The targeted mode of the Markov system in this plot corresponds to a directly decaying mode. The arrow indicates the transition from direct decay to sustained oscillatory dynamics. (d) Phase diagram of system dynamical properties when targeting an oscillatory mode of the Markov system. The arrow highlights the transition from a decaying oscillatory mode to sustained oscillatory dynamics.

in synthetic biology, designing biological circuits capable of sustaining oscillations remains an active area of research [10, 27] and our work shows that additional design criterion is desirable. Our work identifies the strategy for a chemical system coupled to another degree of freedom (Eq. 7-8). Designing such coupled systems may benefit from optimal control strategies that minimize the error between the predicted and targeted oscillatory trajectories with minimum dissipation [28], ensuring precise control of oscillation period and amplitude. Advanced AI-driven tools, such as neural ODEs in optimal control [29], provide powerful methods for handling time-varying target signals in oscillator design, especially for systems with unknown eigenvalues and eigenvectors.

Ultimately, biological oscillators are limit cycles, as they not only maintain a desired frequency but also enforce a fixed amplitude, which is essential for biological functions like heartbeat regulation. Additionally, robustness of biochemical systems to intrinsic and extrinsic noise is crucial for maintaining an accurate period, which depends on the structure of the chemical reaction network and the transition rates at each step [30, 31]. while our model accounts for intrinsic noise (copy number fluctuations) through the chemical master equation, we do not consider extrinsic noise [32]. For systems exhibiting limit cycles, small perturbations due to extrinsic noise should dissipate over time, ensuring robust oscillatory behavior. Future work should incorporate both nonlinearity and extrinsic noise to study the robustness of oscillations under real-world perturbations.

Acknowledgments - This work has been funded in part by NIH R01GM134542. We would like to thank Noah J. Cowan for helpful discussions.

[1] A. T. Winfree, Journal of theoretical biology **16**, 15 (1967).
[2] A. Goldbeter et al., Biochemical Oscillations and Cellular Rhythms (1997).
[3] K. Kruse and F. Jülicher, Current opinion in cell biology **17**, 20 (2005).

[4] V. A. Maltsev, T. M. Vinogradova, and E. G. Lakatta, Journal of pharmacological sciences **100**, 338 (2006).
[5] M. Malumbres and M. Barbacid, Nature reviews cancer **9**, 153 (2009).
[6] J. E. Ferrell, T. Y.-C. Tsai, and Q. Yang, Cell **144**, 874 (2011).
[7] D. Gonze, J.-C. Leloup, and A. Goldbeter, Comptes Rendus de l'Académie des Sciences-Series III-Sciences de la Vie **323**, 57 (2000).
[8] M. J. Rust, S. S. Golden, and E. K. O'Shea, science **331**, 220 (2011).
[9] S. Mukherji and A. Van Oudenaarden, Nature Reviews Genetics **10**, 859 (2009).
[10] M. A. English, R. V. Gayet, and J. J. Collins, Annual Review of Biochemistry **90**, 221 (2021).
[11] B. Novák and J. J. Tyson, Nature reviews Molecular cell biology **9**, 981 (2008).
[12] D. B. Forger (2024).
[13] D. A. McQuarrie, Journal of applied probability **4**, 413 (1967).
[14] J. Keizer, Journal of Statistical Physics **6**, 67 (1972).
[15] D. T. Gillespie, Physica A: Statistical Mechanics and its Applications **188**, 404 (1992).
[16] D. T. Gillespie, The journal of physical chemistry **81**, 2340 (1977).
[17] S. X. Sun, Physical review letters **96**, 210602 (2006).
[18] D. Schnoerr, G. Sanguinetti, and R. Grima, The Journal of Chemical Physics **143** (2015).
[19] A. Ale, P. Kirk, and M. P. Stumpf, The Journal of chemical physics **138** (2013).
[20] A. Sukys and R. Grima, Bioinformatics **38**, 289 (2022).
[21] R. Lefever, G. Nicolis, and P. Borckmans, Journal of the Chemical Society, Faraday Transactions 1: Physical Chemistry in Condensed Phases **84**, 1013 (1988).
[22] M. Nelson and J. Rinzel, The book of genesis **2** (1995).
[23] M. Morari, IEEE Transactions on Automatic Control **30**, 574 (1985).
[24] T. Y.-C. Tsai, Y. S. Choi, W. Ma, J. R. Pomerening, C. Tang, and J. E. Ferrell Jr, Science **321**, 126 (2008).
[25] L. G. Morelli and F. Jülicher, Physical review letters **98**, 228101 (2007).
[26] G. B. Ermentrout, D. H. Terman, G. B. Ermentrout, and D. H. Terman, Mathematical foundations of neuroscience pp. 1–28 (2010).
[27] Z. Zhou, Y. Liu, Y. Feng, S. Klepin, L. S. Tsimring, L. Pillus, J. Hasty, and N. Hao, Science **380**, 376 (2023).
[28] Y. Zhang, Q. Ouyang, and Y. Tu, Physical Review Letters **134**, 018001 (2025).
[29] L. Böttcher, N. Antulov-Fantulin, and T. Asikis, Nature communications **13**, 333 (2022).
[30] C. Del Junco and S. Vaikuntanathan, Physical Review E **101**, 012410 (2020).
[31] C. Del Junco and S. Vaikuntanathan, The Journal of Chemical Physics **152** (2020).
[32] L. S. Tsimring, Reports on Progress in Physics **77**, 026601 (2014).